Universal photonic quantum computation via time-delayed feedback

Hannes Pichler[a,b,1,2], Soonwon Choi[b,1], Peter Zoller[c,d], and Mikhail D. Lukin[b]

[a]Institute for Theoretical Atomic, Molecular and Optical Physics, Harvard-Smithsonian Center for Astrophysics, Cambridge, MA 02138; [b]Department of Physics, Harvard University, Cambridge, MA 02138; [c]Institute for Theoretical Physics, University of Innsbruck, A-6020 Innsbruck, Austria; [d]Institute for Quantum Optics and Quantum Information, Austrian Academy of Sciences, A-6020 Innsbruck, Austria

Edited by Harry J. Kimble, California Institute of Technology, Pasadena, CA, and approved September 19, 2017 (received for review June 18, 2017)

We propose and analyze a deterministic protocol to generate two-dimensional photonic cluster states using a single quantum emitter via time-delayed quantum feedback. As a physical implementation, we consider a single atom or atom-like system coupled to a 1D waveguide with a distant mirror, where guided photons represent the qubits, while the mirror allows the implementation of feedback. We identify the class of many-body quantum states that can be produced using this approach and characterize them in terms of 2D tensor network states.

quantum optics | delayed feedback | photonic quantum computation

Quantum information processing with optical photons is being actively explored for the past two decades (1, 2). However, despite a number of conceptual (3) and technological breakthroughs (4–6), the probabilistic nature of quantum gates limits the scalability of linear optical systems. Here we show that one can deterministically generate photonic states with the full power of universal quantum computation using quantum control of a single emitter in combination with time-delayed coherent quantum feedback (7–9). Our approach is motivated by recent experimental progress demonstrating high-fidelity generation of single photons (5, 10) and deterministic quantum operations between single photons and emitters (11–13) in various systems (14–19). We present an explicit protocol to create a 2D cluster state (20) with a single atomic or atom-like emitter coupled to photonic waveguide. The delayed feedback is introduced by reflecting part of the emitted light field back onto the emitter. Our approach allows for deterministic generation of complex photonic entangled states and opens avenues to photonic quantum computation and quantum simulation using minimal resources already available in current state-of-the-art experiments.

Time-delayed feedback is a powerful tool in several areas of science and engineering (7). In what follows, we show that delayed coherent quantum feedback can be used as a resource to generate quantum entanglement and already in its most basic form may enable universal quantum computation. We focus on quantum optical systems, where it was shown previously that multipartite entanglement between photonic qubits can be generated by a single emitter in a sequential emission process (21–23). We demonstrate that the entanglement structure of the resultant state can be qualitatively enriched using time-delayed quantum feedback. While photons emitted in a generic sequential process are entangled only in a one-dimensional way, characterized by so-called matrix product states (MPSs) (24), we show below that delayed feedback leads to a higher dimensional entanglement structure captured by so-called projected entangled pair states (PEPSs) (25). Significantly, while MPSs have limited use for quantum computation and simulation, as they can be efficiently simulated classically, PEPSs contain states that serve as a resource for universal measurement-based quantum computation (MBQC) (20). The difference is rooted in the Markovian nature of the sequential emission process that severely restricts the class of achievable states. In contrast, time-delayed quantum feedback renders the system non-Markovian, introducing an effective quantum memory that we harness to create a universal resource. While previous works proposed compensating for this limitation of Markovian systems by using multiple quantum emitters (22), we stress that delayed feedback allows for enabling photonic MBQC already with a single emitter.

Photonic 2D Cluster State

The fundamental building block of our approach is a single, driven quantum emitter ($\mathcal{Q}$) coupled to a 1D waveguide and a distant mirror as depicted in Fig. 1*A*. Our protocol consists of a repeated excitation of this quantum emitter, leading to an emission of a train of photon pulses into the waveguide, encoding qubits via the absence ($|0\rangle_k$) or presence ($|1\rangle_k$) of a photon in the k-th pulse. The mirror feeds these photons back to the emitter with a time delay τ, such that the photons can interact with the emitter more than once (Fig. 1*B*). In this way, the emitter can create correlations not only between subsequently emitted photons but also between photon pulses separated by the time delay τ. Effectively this leads to a two-dimensional entanglement structure as we discuss now for the specific example of the 2D cluster state (see also Fig. 1*C*).

For concreteness, we focus on an emitter (representing $\mathcal{Q}$) with an internal structure depicted in Fig. 2*A*, supporting two metastable states $|g_1\rangle \equiv |0\rangle_{\mathcal{Q}}$ and $|g_2\rangle \equiv |1\rangle_{\mathcal{Q}}$, which can be coherently manipulated by a classical field $\Omega_1(t)$. The emitter can be excited from $|g_2\rangle$ to a state $|e_L\rangle$ using a laser with Rabi frequency $\Omega_2(t)$. Following each excitation, the atom will decay to

Significance

Creating large entangled states with photons as quantum information carriers is a central challenge for quantum information processing. Since photons do not interact directly, entangling them requires a nonlinear element. One approach is to sequentially generate photons using a quantum emitter that can induce quantum correlations between photons. Here we show that delayed quantum feedback dramatically expands the class of achievable photonic quantum states. In particular, we show that in state-of-the-art experiments with single atom-like quantum emitters, the most basic form of delayed quantum feedback already allows for creation of states that are universal resources for quantum computation. This opens avenues for quantum information processing with photons using minimal experimental resources.

Author contributions: H.P., S.C., P.Z., and M.D.L. designed research; H.P. and S.C. performed research; H.P. and S.C. analyzed data; and H.P., S.C., P.Z., and M.D.L. wrote the paper.

The authors declare no conflict of interest.

This article is a PNAS Direct Submission.

[1]H.P and S.C. contributed equally to this work.

[2]To whom correspondence should be addressed. Email: hannes.pichler@cfa.harvard.edu.

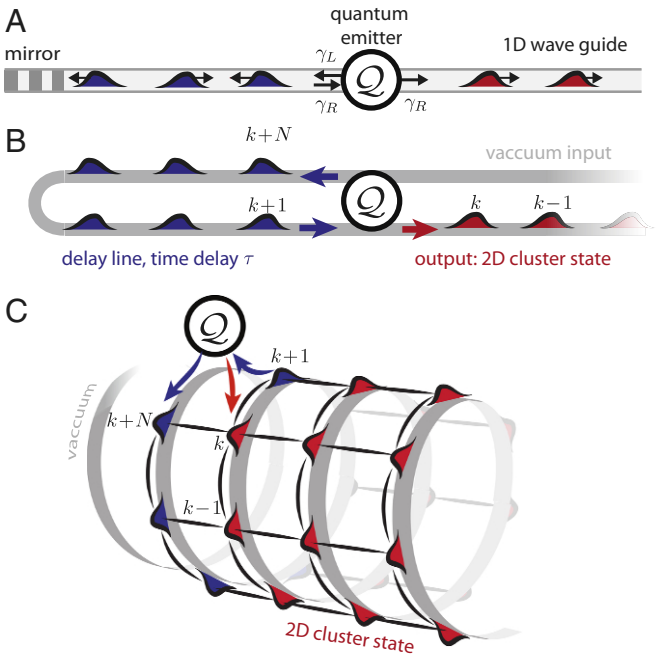

Fig. 1. Schematic setting. (*A*) A quantum emitter $\mathcal{Q}$ is coupled to a 1D waveguide that is terminated on one side by a (distant) mirror. (*B*) In each time step k, $\mathcal{Q}$ can emit a phtoton ($k+N$) toward the mirror—that is, into a delay line—and interact with a photon k returning from the delay line, exiting at the output port. (*C*) Visualization of the resulting entanglement structure: Wrapping the photon channel displayed in *B* around a cylinder with the proper circumference (equivalent to the time delay τ), it can be seen that in each time step $\mathcal{Q}$ interacts with two photons that are neighboring along the artificial, second dimension. Therefore, as time progresses, $\mathcal{Q}$ creates entanglement between neighboring photonic qubits, both in the physical and the artificial dimension.

$|g_2\rangle$, emitting a photon into the waveguide. For now, we assume that the atom–photon coupling is chiral (26) such that every such photon is emitted unidirectionally—that is, to the left in Fig. 1*A* (see however below). Finally, another excited state $|e_R\rangle$, degenerate with $|e_L\rangle$, couples to the right, moving photons reflected from the mirror. We denote the corresponding decay rates by γ_L and γ_R.

Protocol. Our protocol starts by first generating 1D cluster states of left-propagating photons (21). To this end, the atom is initially prepared in the state $|0\rangle_{\mathcal{Q}}$. Then, a rapid $\pi/2$ pulse is applied on the atomic qubit, followed by a π pulse on the $|g_2\rangle \to |e_L\rangle$ transition (Fig. 2 *A* and *B*). The subsequent decay from state $|e_L\rangle$ to $|g_2\rangle$ results in entanglement between the atom and the emitted photon—that is, $|0\rangle_{\mathcal{Q}}|0\rangle_1 + |1\rangle_{\mathcal{Q}}|1\rangle_1$. Repeating this pulse sequence for n times leads to a train of photonic qubits in the form of a 1D cluster state. An analogous scheme has been demonstrated in an experiment using a quantum dot (23), following a seminal proposal by Lindner and Rudolph (21).

Remarkably, the 2D cluster state is generated from exactly the same sequence if we take into account the effect of the mirror and the scattering of the reflected photons from the atom. We are interested in the situation where the time delay τ is so large that the k-th photon interacts for the second time with the atom between the generation of the $(k+N-1)$-th and $k+N$-th photon. This is achieved, for example, by setting $\tau = (N-1/2)T$ (with T the protocol period; see Fig. 2*B*). Crucially, if the atom is then in the state $|g_2\rangle$, the returning photon is resonantly coupled to the $|g_2\rangle \to |e_R\rangle$ transition, picking up a scattering phase shift of π without any reflection (26). In contrast, if the atom is in state $|g_1\rangle$ or the photon mode is empty, there is no interaction. This process implements a controlled σ^z gate

$$\hat{Z}_{\mathcal{Q},k} = |0\rangle_{\mathcal{Q}}\langle 0| \otimes \mathbb{1}_k + |1\rangle_{\mathcal{Q}}\langle 1| \otimes \sigma_k^z \qquad [1]$$

entangling the atom and the k-th photon. In turn, the subsequently generated $k+N$-th photon inherits this entanglement, thereby giving rise to an effective 2D entanglement structure (Fig. 1*C*).

Formally, the protocol can be interpreted as a sequential application of gates $\hat{X}_{\mathcal{Q},k+N}\hat{Z}_{\mathcal{Q},k}\hat{H}_{\mathcal{Q}}$, on the atom and photonic qubits k and $k+N$, on the initial trivial state $|0\rangle_{\mathcal{Q}} \bigotimes_k |0\rangle_k$ (Fig. 2 *C* and *D*). Here $\hat{H}_{\mathcal{Q}} = \frac{1}{\sqrt{2}}(\sigma^z_{\mathcal{Q}} + \sigma^x_{\mathcal{Q}})$ and $\hat{X}_{\mathcal{Q},k} = |0\rangle_{\mathcal{Q}}\langle 0| \otimes \mathbb{1}_k + |1\rangle_{\mathcal{Q}}\langle 1| \otimes \sigma^x_k$. One can show that after $(M+1)\times N$ turns, this gives exactly the 2D cluster state on a $M \times N$ square lattice with shifted periodic boundary conditions (see *Materials and Methods*):

$$|\psi_{C_{2D}}\rangle = \left(\prod_{k=1}^{N(M+1)} \hat{X}_{\mathcal{Q},k+N}\hat{Z}_{\mathcal{Q},k}\hat{H}_{\mathcal{Q}}\right)|0\rangle_{\mathcal{Q}} \bigotimes_k |0\rangle_k. \qquad [2]$$

Universal quantum computation (27) can be performed by sequentially measuring each photonic qubit directly at the output port—for example, using another atom as a high-fidelity measurement device. This can be implemented using pulse shaping techniques (Fig. 3*A*), allowing for a perfect absorption of each photon by the second atom (28, 29).

Experimental Requirements. Photons generated in this pulsed scheme have a finite bandwidth $\mathcal{B}$. To realize the controlled phase gate given in Eq. **1**, this bandwidth must be small—that is, $\mathcal{B} \ll \gamma_R$ (26); otherwise, the wave packet is distorted when scattered by the atom, reducing the gate fidelity, $\mathcal{F}_Z$ (Fig. 3*C*). Narrow-bandwidth photons and high-fidelity gates can be obtained by shaping the temporal profiles, eliminating the error to first order

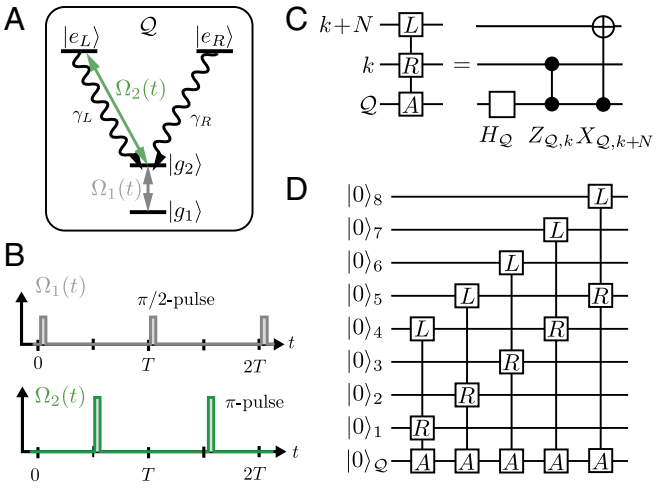

Fig. 2. Protocol to generate the photonic 2D cluster state. With the level structure (*A*) and periodic, pulsed coherent drive (*B*), the setup in Fig. 1*A* leads to a 2D cluster state of photons in the output. During each step $k = 1, 2, \ldots$ (of duration T), the pulse (*B*) sequence realizes a unitary involving the emitter $\mathcal{Q}$ (*A*) and two photonic qubits, k and $k+N$ [realized by a right (*R*) and left (*L*) moving photon, respectively], with $N = 3$ in *D*. The corresponding circuit diagram is shown in *C* and *D*. Each step consists of a Hadamard gate $\hat{H}_{\mathcal{Q}}$ and a controlled phase gate $\hat{Z}_{\mathcal{Q},k}$ between the atom and the photon qubit k returning from the delay line, followed by a controlled-NOT gate $\hat{X}_{\mathcal{Q},k+N}$ (see Eq. **2**).

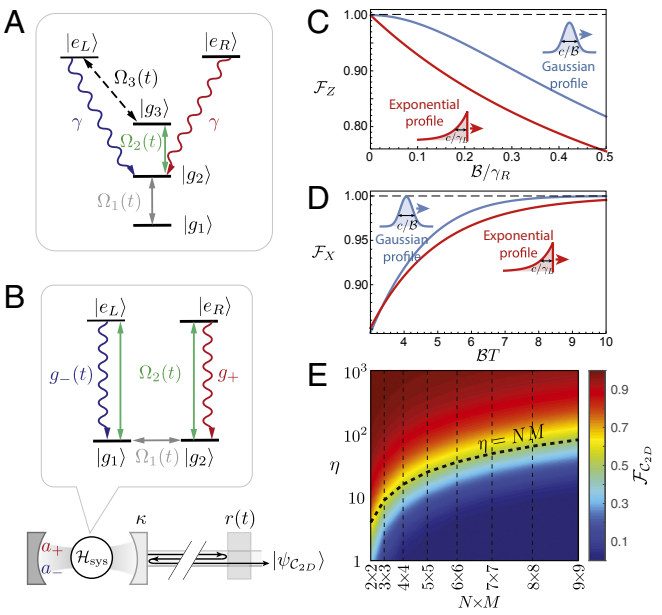

Fig. 3. Modified setups and effects of imperfections. (*A*) Exciting the atom via a third stable state $|g_3\rangle$ in a Raman-type configuration, one can shape the profile of the emitted photon wave-packet. In the limit $|\Omega_3(t)| \ll \gamma$, an adiabatic elimination of the excited state $|e_L\rangle$ leads to the same effective dynamics as in Fig. 2*B*, but with a renormalized and dynamically controllable, effective decay rate $\gamma_L(t) = |\Omega_3(t)|^2/(2\gamma)$. (*B*) Modified setup to generate the 2D cluster state in a cavity QED setting with photon qubits encoded in polarization degrees of freedom and without the requirement of chiral coupling. (*C*) Fidelity of the controlled phase gate for a photon with Lorentzian (red) or Gaussian (blue) spectrum (see also *Materials and Methods*). (*D*) Analogously, fidelity of photon generation as a function of the protocol period T. (*E*) Effect of photon loss: Fidelity of the generated state ρ (with $\eta_L = \eta_R = \eta$) and the 2D cluster states of size $N \times M$, $\mathcal{F}_{c_{2D}} = \sqrt{\langle\psi_{c_{2D}}|\rho|\psi_{c_{2D}}\rangle}$.

in $\mathcal{B}/\gamma_R$ (Fig. 3*C* and *Materials and Methods*). We note that dispersive distortions due to photon propagation can be absorbed in a redefinition of the qubit states and do not affect the resulting state.

Second, the information capacity of the feedback loop is bounded by the number of photons in the delay line, N. To well distinguish two consecutive photons, one can only generate them at a rate $1/T \ll \mathcal{B}$ (see Fig. 3*D*). Therefore, the requirement for narrow-bandwidth photons is competing with the effective size of the emergent, second dimension N. This gives rise to the hierarchy $N \sim \tau/T \ll \tau\mathcal{B} \ll \gamma_R\tau$ required for a high-fidelity implementation of our protocol. Therefore, the required length of the delay line $\ell = \frac{\tau c}{2n_g}$ scales as $\ell \sim \frac{Nc}{2\gamma_R n_g}$, where c is the speed of light and n_g the refractive index in the waveguide. In the optical domain—for example, using single quantum dots (15) or neutral atoms (13) with typical emission rates in the GHz regime—this leads to a length of $\ell \sim \frac{N}{n_g} \times 10^{-1}$ m. Note that τ (ℓ) can be dramatically enhanced (reduced)—for example, via a dispersive slow-light medium (30) or techniques based on electromagnetically induced transparency (31). At microwave frequencies, using superconducting qubits as quantum emitters, long delay lines can be realized by exploiting the slow propagation speed of surface acoustic waves (32).

Apart from these fundamental considerations, experimental imperfections will eventually limit the achievable size of the cluster state. One of the most important challenges is photon loss (33) in atom–photon interactions, often quantified by the so-called cooperativity $\eta_j = \gamma_j/\Gamma_j$ ($j = L, R$), where Γ_j denotes emission rate into unguided modes from state $|e_j\rangle$. Amplitude attenuation in the waveguide (with attenuation length κ) can be accounted for by an effective cooperativity $\eta_L = \gamma_L/\Gamma_L e^{-2\ell/\kappa}$. Large, high-fidelity cluster states can be obtained in the regime $\eta_j \gg 1$, where the achievable system sizes scale as $NM \lesssim (1/\eta_L + 2/\eta_R)^{-1}$ (Fig. 3*E*). High cooperativities have been demonstrated in nanophotonic experiments with neutral atoms and solid-state emitters (13, 15).

Finally, we note that chiral coupling is not essential in realizing the above protocol. For example, in a cavity QED setting (12, 13), the delayed feedback can be introduced by a distant, switchable mirror (Fig. 3*B*). There, proper control of the mirror can ensure that each generated photon interacts exactly twice with the emitter. Moreover, in such a setting one can encode qubit states in photon polarizations rather than number of degrees of freedom, allowing the detection of photon loss errors.

Theory

In this section, we discuss the generation of 2D entangled photonic states using delayed quantum feedback from a more general perspective. We still consider the paradigmatic setup of delayed quantum feedback in Fig. 1*A* but now study arbitrary protocols that can be realized in such a setting. We completely characterize the class of photonic quantum states that can be generated in this setup in terms of PEPSs. This establishes a remarkable connection between non-Markovian quantum optical systems and condensed matter theory, where PEPSs appear naturally in the description of correlated many-body quantum systems in higher dimensions (25).

To this end, we turn to a more abstract description of the dynamics depicted in Fig. 1 (see also *Materials and Methods*). Formally, the quantum system $\mathcal{Q}$ generates an output state by sequential unitary interaction with two qubits k and $k+N$ on a 1D array, representing the photonic qubits. Assuming that the qubits are initialized in the state $|0\rangle$, this process is descried by a map:

$$\hat{U}[k] = \sum_{i,a,b,c,d} U[k]^i_{a,b,c,d} |i,a,b\rangle\langle c,0,d|, \qquad [3]$$

where $|i,a,b\rangle \equiv |i\rangle_k |a\rangle_{k+N} |b\rangle_{\mathcal{Q}}$ denotes a state with k-th and $k+N$-th qubits and $\mathcal{Q}$ in states i, a, and b, respectively. Repeated application of such maps produces a quantum state $|\Psi(k)\rangle$, describing $\mathcal{Q}$ and the string of photonic qubits after k steps:

$$|\Psi(k)\rangle = \hat{U}[k]|\Psi(k-1)\rangle = \prod_{j=1}^{k} \hat{U}[j]|\Psi(0)\rangle. \qquad [4]$$

Given the initial state, the wavefunction is entirely specified by the tensors $U[j]^i_{a,b,c,d}$ ($j = 1 \ldots k$), and in particular, it can be expressed as a contraction of the 2D tensor network shown in Fig. 4*B* (see also *Materials and Methods*). Generating specific 2D tensor network states of photons can thus be achieved by proper design of the protocol, corresponding to the tensors $U^i_{a,b,c,d}$. The unitarity of the dynamics requires the tensors to satisfy

$$\sum_{i,a,b} U^i_{a,b,c,d} \left(U^i_{a,b,c',d'}\right)^* = \delta_{c,c'}\delta_{d,d'}. \qquad [5]$$

Physically, this isometric condition reflects the deterministic and sequential nature of the protocol. Importantly, every 2D tensor network state (or PEPS) that can be brought into a form respecting Eq. **5** can be constructed in this setting with a single quantum emitter and delayed feedback. Per construction, we showed that this includes universal resources for MBQC, but it also allows for designing protocols to create exotic 2D states of light, exhibiting topological order such as string-net states (34) or the ground state of Kitaev's toric code Hamiltonian (35) (see *Materials and Methods*).

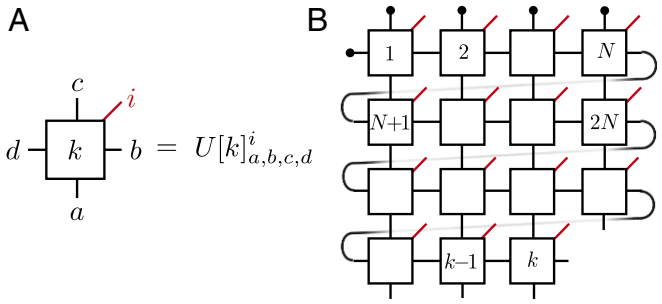

Fig. 4. Tensor network representation of the generated states. (*A*) Graphical representation of the rank-5 tensors $U[k]^i_{a,b,c,d}$. The "physical index" i denotes the state of the qubit k, the "horizontal bonds" b and d run over internal degrees of freedom of $\mathcal{Q}$, and "vertical bonds" a and c enumerate the quantum states of input into and output from the delay line, respectively. (*B*) Representation of the state Eq. **4** in terms of these tensors. Connected lines indicate contractions, and red open lines denote physical indices corresponding to the states of qubits in the output. In the top row, the tensors are contracted with the initial state of $\mathcal{Q}$ and the vacuum state for the first N qubits in the string, as indicated by the black circles. Open legs at the bottom correspond to the state of the qubits in the delay line after step k, and the open line on the bottom right corresponds to the state of $\mathcal{Q}$.

We finally note that this possibility of creating PEPSs as output states of delayed feedback schemes allows for developing variational photonic quantum simulators of strongly correlated 2D systems, extending recently implemented proposals for 1D systems (18, 36) to higher dimensions. This is particularly important, since unlike in 1D, quantum simulators in higher dimensions cannot be efficiently simulated by classical computers.

Outlook

Our work can be extended in several ways, including the addition of multiple delay lines, leading to tensor networks in higher dimensions. This is of relevance for fault-tolerant implementations of MBQC using 3D cluster states (20). Additionally, on can envisage implementing variants of MBQC that can tolerate up to 50% of counterfactual errors due to photon loss (37). Finally, besides nanophotonic setups, our "single-atom quantum computer" can be implemented in a circuit QED system with microwave photons (16, 18), surface-acoustic, or bulk-acoustic waves (32, 38).

Materials and Methods

2D Cluster State Representation. In this section, we prove that $|\psi_{C_{2D}}\rangle$ in Eq. **3** represents the 2D cluster state. To this end, we start first with the representation of the 1D cluster state on $K+1$ qubits:

$$|\psi_{C_{1D}}\rangle = \prod_{k=1}^{K} Z_{k,k+1}|+\rangle^{\otimes K+1}. \quad [6]$$

Using the swap operator $S_{i,j}$ that exchanges the quantum states of qubits i and j, we can rewrite the 1D cluster state as

$$|\psi_{C_{1D}}\rangle = \left(\prod_{k=1}^{K} S_{\mathcal{Q},k} Z_{\mathcal{Q},k}\right)|+\rangle_{\mathcal{Q}} \bigotimes_{k=1}^{K} |+\rangle_k \quad [7]$$

where we used the relation $Z_{b,c} = S_{a,b} Z_{a,c} S_{a,b}$ and identified the $K+1$th qubit with the ancilla $\mathcal{Q}$. Note that throughout this paper, we use a convention where the ordering in the product is defined via $\prod_{j=1}^{k} M_j = M_k M_{k-1} \ldots M_1$. We now use the relation

$$S_{\mathcal{Q},v} Z_{\mathcal{Q},v} |\psi\rangle_{\mathcal{Q}} \otimes |+\rangle_v = H_{\mathcal{Q}} X_{\mathcal{Q},v} H_v |\psi\rangle_{\mathcal{Q}} \otimes |+\rangle_v, \quad [8]$$

where H_x is the Hadamard gate acting on qubit x. We note that this equality is not an operator identity but a property of states of the form $|\psi\rangle_{\mathcal{Q}} \otimes |+\rangle_v$, where the qubit v must be in the state $|+\rangle_v$ while the ancillary system $|\psi\rangle_{\mathcal{Q}}$ may be in an arbitrary state, potentially entangled to other systems. Using these relations, our state can be written as:

$$|\psi_{C_{1D}}\rangle = \left(\prod_{k=1}^{K} H_{\mathcal{Q}} X_{\mathcal{Q},k}\right)|+\rangle_{\mathcal{Q}} \bigotimes_{k=1}^{K} |0\rangle_k. \quad [9]$$

We note that this representation of the 1D cluster state has been also used in ref. 21.

We now proceed to the construction of the 2D cluster state. From its definition, the 2D cluster state can be obtained from the 1D cluster state above by introducing additional entanglement (via phase gates) between qubits k and $k+N$ (27). This gives a 2D cluster state on a square lattice with shifted periodic boundary conditions, where the extend of the (shifted) periodic direction is set by N.

$$\begin{aligned} |\psi_{C_{2D}}\rangle &= \left(\prod_{k=N+1}^{K} Z_{k,k-N}\right)\left(\prod_{k=1}^{K} H_{\mathcal{Q}} X_{\mathcal{Q},k}\right)|+\rangle_{\mathcal{Q}} \bigotimes_{k} |0\rangle_k \\ &= \left(\prod_{k=1}^{K} H_{\mathcal{Q}} Z_{k,k-N} X_{\mathcal{Q},k}\right)|+\rangle_{\mathcal{Q}} \bigotimes_{k} |0\rangle_k. \end{aligned} \quad [10]$$

In the second line, we used the fact that $[Z_{j,j+N}, X_{\mathcal{Q},k}] = 0$ for $j > k$, and $Z_{k,j}|0\rangle_j = \mathbb{1}_k \otimes \mathbb{1}_j |0\rangle_j$. Now we make use of the identity

$$Z_{n,m} X_{\mathcal{Q},n} |\psi\rangle_{\mathcal{Q},m} |0\rangle_n = X_{\mathcal{Q},n} Z_{\mathcal{Q},m} |\psi\rangle_{\mathcal{Q},m} |0\rangle_n, \quad [11]$$

where $|\psi\rangle_{\mathcal{Q},m}$ is an arbitrary state of $\mathcal{Q}$ and every qubit including $m \neq n$ but not n. Again, this relation is not an operator identity but a property of a state where qubit n is in the separable state $|0\rangle_n$. Using this identity, we arrive at

$$|\psi_{C_{2D}}\rangle = \left(\prod_{k=1}^{K} H_{\mathcal{Q}} X_{\mathcal{Q},k} Z_{\mathcal{Q},k-N}\right)|+\rangle_{\mathcal{Q}} \bigotimes_{k} |0\rangle_k \quad [12]$$

which is (up to a shift of the index and a rotation of $\mathcal{Q}$) exactly our protocol given in Eq. **3**.

General Entanglement Structure. In this section, we provide details on the explicit connection between the class of achievable states from using a single emitter with delayed quantum feedback and 2D tensor network states (PEPS). To this end, we use induction to show that the repeated application of $\hat{U}[k]$ in Eq. **4** results in a 2D tensor network that "grows" by an additional tensor in each time step (Fig. 4*B*). This can be seen by induction: we assume that the quantum state of the system after $k-1$ steps can be written as

$$|\Psi(k-1)\rangle \otimes |0\rangle = \sum_{i_{\mathcal{Q}},\{i_j\}} \mathcal{C}[k-1]^{i_{\mathcal{Q}},\{i_j\}} |i_{\mathcal{Q}},\{i_j\}\rangle \otimes |0\rangle, \quad [13]$$

where $|0\rangle$ is the input state of the $k+N$-th qubit (Fig. 1*B*) and $\mathcal{C}[k-1]^{i_{\mathcal{Q}},\{i_j\}}$ denotes the contraction of the 2D tensor network formed by $U[\ell]$ ($\ell \in \{1, \cdots, k-1\}$) in Fig. 4*B* with open indices $i_{\mathcal{Q}}$, $\{i_j\}$. The basis state $|i_{\mathcal{Q}}, \{i_j\}\rangle$ enumerates configurations of $\mathcal{Q}$ and the array of $k-1$ output qubits ($j \in \{1, \cdots, k-1\}$) and N memory qubits in the delay line ($j \in \{k, \cdots, k+N-1\}$). The application of $\hat{U}[k]$ in the k-th step modifies the quantum state of k-th and $k+N$-th qubits and $\mathcal{Q}$. From Eqs. **3** and **4**, new quantum amplitude $A_{i_{\mathcal{Q}},\{i_j\}}$ for a configuration $|i_{\mathcal{Q}}, \{i_j\}\rangle$ can be written as

$$\begin{aligned} A_{i_{\mathcal{Q}},\{i_j\}} &= \sum_{i'_{\mathcal{Q}},\{i'_j\}} U[k]^{i_k}_{i_{k+N},i_{\mathcal{Q}},i'_k,i'_{\mathcal{Q}}} \prod_{j \notin \mathcal{Q},k} \delta_{i_j,i'_j} \mathcal{C}[k-1]^{i'_{\mathcal{Q}},\{i'_j\}} \\ &= \mathcal{C}[k]^{i_{\mathcal{Q}},\{i_j\}}, \end{aligned} \quad [14]$$

where the second line is achieved by identifying $U[k]^{i_k}_{i_{k+N},i_{\mathcal{Q}},i'_k,i'_{\mathcal{Q}}}$ as a rank-5 tensor in Fig. 4*A* and by realizing that the summations over i'_k and $i'_{\mathcal{Q}}$ are equivalent to the contraction of vertical and horizontal bonds of newly introduced tensor $U[k]$, respectively (see Fig. 4*B*). We note that the generated network in Fig. 4*B* is contracted with shifted periodic boundary conditions.

This inductive construction also shows that the arbitrary 2D tensor network satisfying Eq. **5** can be generated from our method via appropriate choice of unitary $\hat{U}[k]$. Interestingly, this class of states includes exotic states with topological order such as string-net states (34) or the ground state of Kitaev's Hamiltonian (35). For example, the latter state can be represented by a 2D network of translationally invariant tensors $U^{i_1,i_2,i_3,i_4}_{a,b,c,d} = \delta_{a+b,i_1}\delta_{d+a,i_2}\delta_{c+d,i_3}\delta_{b+c,i_4}/4$, where $i_1, \ldots, i_4$ denote the states of four physical qubits in a unit cell and $\{a, b, c, d\}$ run over bond dimension 2. This tensor explicitly satisfies Eq. **5** and can immediately be translated into a protocol similar to the one for generating the 2D cluster state—that is, using only controlled single photon generation and atom–photon phase gates between that atom and feedback photons.

Imperfections. Without shaping the wave packets of the emitted photons, each photon produced in a single step has a Lorentzian spectral profile, whose temporal profile is

$$f(t) = \sqrt{\gamma_L} e^{-\gamma_L t/2}\Theta(t) = i\int d\omega\, \frac{2\pi}{\sqrt{\gamma_L}} \frac{1}{\omega + i\gamma_L/2} e^{-i\omega t} \qquad [15]$$

where we chose a normalization $\int dt|f(t)|^2 = 1$. The scattering phase shift for the chiral forward scattering (if the atom is in state $|g_2\rangle$) is determined by the transmission:

$$t(\omega) = \frac{\omega - i\gamma_R/2}{\omega + i\gamma_R/2} \qquad [16]$$

such that the wave packet $f(t)$ transforms into

$$\tilde{f}(t) = i\int d\omega\, \frac{2\pi}{\sqrt{\gamma_L}} \frac{\omega - i\gamma_R/2}{\omega + i\gamma_R/2} \frac{1}{\omega + i\gamma_L/2} e^{-i\omega t} \qquad [17]$$

$$= -\sqrt{\gamma_L}\left(\frac{\gamma_R + \gamma_L}{\gamma_R - \gamma_L} e^{-\gamma_L t/2} - 2\frac{\gamma_R}{\gamma_R - \gamma_L} e^{-\gamma_R t/2}\right)\Theta(t) \qquad [18]$$

It is straightforward to calculate the overlap

$$\int dt f^*(t)\tilde{f}(t) = -\frac{1 - \gamma_L/\gamma_R}{1 + \gamma_L/\gamma_R} \qquad [19]$$

With this, we obtain the fidelity of the controlled phase gate:

$$\mathcal{F}_Z = \frac{2\frac{\gamma_l}{\gamma_R}\left(\frac{\gamma_l}{\gamma_R} + 3\right) + 5}{5\left(\frac{\gamma_l}{\gamma_R} + 1\right)^2} = 1 - \frac{4}{5}\frac{\gamma_L}{\gamma_R} + \mathcal{O}\left(\frac{\gamma_L^2}{\gamma_R^2}\right). \qquad [20]$$

If we shape the coupling via $\gamma_L(t) = \frac{4\Omega^2(t)}{\gamma}$, then $f(t) = \sqrt{\gamma_L(t)}\exp\left(-\int_0^t ds\gamma_L(s)/2\right)$. Pulse shaping allows for creating photon wave packets that are symmetric in time. Straightforward calculation shows that, for example, the Gaussian wave packet

$$f(t) = \sqrt{\mathcal{B}/\sqrt{\pi}} e^{-\mathcal{B}^2(t-t_0)^2/2} \qquad [21]$$

can be obtained by

$$\gamma_L(t) = \frac{2\mathcal{B}e^{-\mathcal{B}^2(t-t_0)^2}}{\sqrt{\pi}(1 - \mathrm{erf}(\mathcal{B}(t - t_0)))}. \qquad [22]$$

The corresponding fidelity of the phase gate can be calculated from

$$\int dt f^*(t)\tilde{f}(t) = 1 - \frac{\sqrt{\pi}e^{\frac{1}{4x^2}}\left(1 - \mathrm{erf}\left(\frac{1}{2x}\right)\right)}{x}$$
$$= -1 + 4x^2 + \mathcal{O}(x^4) \qquad [23]$$

with $x = \mathcal{B}/\gamma_R$ and the Gaussian error function $\mathrm{erf}(z) = \frac{2}{\sqrt{\pi}}\int_0^z dt e^{-t^2}$. This gives the fidelity $\mathcal{F}_Z = 1 - \frac{8}{5}x^2 + \mathcal{O}(x^4)$. We note that the linear order in x vanishes in this expression unlike in the previous case without the shaping of a wave packet. This is a consequence of a temporally symmetric wave packet, which can significantly improve the fidelity.

In the proposed implementation to create the 2D cluster state, the gate $\hat{X}_{\mathcal{Q},k+N}$ is realized by emission of a photon associated with the transition $|e_L\rangle \to |g_2\rangle$ during the second half of each time step with period T. In order for the gate $\hat{X}_{\mathcal{Q},k+N}$ to work, we thus require $T/2$ to be much larger than the temporal extend of the emitted photon; otherwise, the next step in our protocol would proceed even before the gate $\hat{X}_{\mathcal{Q},k_N}$ is completed, leading to an error. The fidelity for this process can computed from the quantity

$$\epsilon = \int_{t_0}^{t_0+T/2} dt\gamma_L(t)\exp\left(-\int_0^t ds\gamma_L(s)\right) \qquad [24]$$

via $\mathcal{F}_X = 1 - \frac{2}{3}\epsilon + \frac{1}{6}\epsilon^2$. Without shaping the photon wave packet—that is, with $\gamma_L(t) = \gamma_L$ as in Eq. **15**—one gets $\epsilon = e^{-\gamma_L T/2}$, while for the pulse-shaped photon Eq. **22** (with $t_0 = -T/4$) we find $\epsilon = 1 - \sqrt{2}\frac{\mathrm{erf}(\mathcal{B}T/4)}{\sqrt{1+\mathrm{erf}(\mathcal{B}T/4)}}$.

For large $x = \mathcal{B}T/4 \gg 1$, we have $\epsilon \to e^{-x^2}/(\sqrt{\pi}x)$. In both cases, the gate fidelity approaches 1 exponentially, but in the case of a shaped photon wave packet, this approach is again faster.

ACKNOWLEDGMENTS. We thank J. I. Cirac, J. Haegeman, L. Jiang, N. Schuch, and F. Verstraete for useful discussions. This work was supported through the National Science Foundation (NSF), the Center for Ultracold Atoms, the Air Force Office of Scientific Research via the Multidisciplinary University Research Initiative, and the Vannevar Bush Faculty Fellowship. H.P. is supported by the NSF through a grant for the Institute for Theoretical Atomic, Molecular, and Optical Physics at Harvard University and the Smithsonian Astrophysical Observatory. S.C. acknowledges the support from Kwanjeong Educational Foundation. Work at Innsbruck is supported by the Special Research Program Foundations and Applications of Quantum Science of the Austrian Science Fund, as well as the European Research Council Synergy Grant Ultracold Quantum Matter.

1. Kok P, et al. (2007) Linear optical quantum computing with photonic qubits. *Rev Mod Phys* 79:135–174.
2. Pan JW, et al. (2012) Multiphoton entanglement and interferometry. *Rev Mod Phys* 84:777–838.
3. Knill E, Laflamme R, Milburn GJ (2001) A scheme for efficient quantum computation with linear optics. *Nat Nanotechnol* 409:46–52.
4. Walther P, et al. (2005) Experimental one-way quantum computing. *Nat Nanotechnol* 434:169–176.
5. Ding X, et al. (2016) On-demand single photons with high extraction efficiency and near-unity indistinguishability from a resonantly driven quantum dot in a micropillar. *Phys Rev Lett* 116:020401.
6. Aharonovich I, Englund D, Toth M (2016) Solid-state single-photon emitters. *Nat Photon* 10:631–641.
7. Wiseman HM, Milburn GJ (2010) *Quantum Measurement and Control* (Cambridge Univ Press, Cambridge, UK).
8. Grimsmo AL (2015) Time-delayed quantum feedback control. *Phys Rev Lett* 115:060402.
9. Pichler H, Zoller P (2016) Photonic circuits with time delays and quantum feedback. *Phys Rev Lett* 116:093601.
10. Sipahigil A, et al. (2016) An integrated diamond nanophotonics platform for quantum-optical networks. *Science* 354:847–850.
11. Volz J, Scheucher M, Junge C, Rauschenbeutel A (2014) Nonlinear π phase shift for single fibre-guided photons interacting with a single resonator-enhanced atom. *Nat Photon* 8:965–970.
12. Reiserer A, Kalb N, Rempe G, Ritter S (2014) A quantum gate between a flying optical photon and a single trapped atom. *Nat Nanotechnol* 508:237–240.
13. Tiecke TG, et al. (2014) Nanophotonic quantum phase switch with a single atom. *Nat Nanotechnol* 508:241–244.
14. Goban A, et al. (2014) Atom–light interactions in photonic crystals. *Nat Commun* 5:3808.
15. Söllner I, et al. (2015) Deterministic photon–emitter coupling in chiral photonic circuits. *Nat Nanotechnol* 10:775–778.
16. Hoi IC, et al. (2015) Probing the quantum vacuum with an artificial atom in front of a mirror. *Nat Phys* 11:1045–1049.
17. Stute A, et al. (2013) Quantum-state transfer from an ion to a photon. *Nat Photon* 7:219–222.
18. Eichler C, et al. (2015) Exploring interacting quantum many-body systems by experimentally creating continuous matrix product states in superconducting circuits. *Phys Rev X* 5:041044.
19. Lodahl P, Mahmoodian S, Stobbe S (2015) Interfacing single photons and single quantum dots with photonic nanostructures. *Rev Mod Phys* 87:347–400.
20. Briegel HJ, Browne DE, Dür W, Raussendorf R, Van den Nest M (2009) Measurement-based quantum computation. *Nat Phys* 5:19–26.
21. Lindner NH, Rudolph T (2009) Proposal for pulsed on-demand sources of photonic cluster state strings. *Phys Rev Lett* 103:113602.
22. Economou SE, Lindner N, Rudolph T (2010) Optically generated 2-dimensional photonic cluster state from coupled quantum dots. *Phys Rev Lett* 105:093601.
23. Schwartz I, et al. (2016) Deterministic generation of a cluster state of entangled photons. *Science* 354:434–437.
24. Schön C, Solano E, Verstraete F, Cirac JI, Wolf MM (2005) Sequential generation of entangled multiqubit states. *Phys Rev Lett* 95:110503.
25. Verstraete F, Cirac JI (2004) Renormalization algorithms for quantum-many body systems in two and higher dimensions. arXiv.org pp. cond–mat–0407066.
26. Lodahl P, et al. (2017) Chiral quantum optics. *Nat Nanotechnol* 541:473–480.
27. Raussendorf R, Briegel HJ (2001) A one-way quantum computer. *Phys Rev Lett* 86:5188–5191.
28. Cirac JI, Zoller P, Kimble HJ, Mabuchi H (1997) Quantum state transfer and entanglement distribution among distant nodes in a quantum network. *Phys Rev Lett* 78: 3221–3224.
29. Pechal M, et al. (2014) Microwave-controlled generation of shaped single photons in circuit quantum electrodynamics. *Phys Rev X* 4:041010.
30. Baba T (2008) Slow light in photonic crystals. *Nat Photon* 2:465–473.
31. Fleischhauer M, Imamoglu A, Marangos J (2005) Electromagnetically induced transparency: Optics in coherent media. *Rev Mod Phys* 77:633–673.
32. Gustafsson MV, et al. (2014) Propagating phonons coupled to an artificial atom. *Science* 346:207–211.
33. Nutz T, Milne A, Shadbolt P, Rudolph T (2017) Proposal for demonstration of long-range cluster state entanglement in the presence of photon loss. *APL Photon* 2:066103.
34. Buerschaper O, Aguado M, Vidal G (2009) Explicit tensor network representation for the ground states of string-net models. *Phys Rev B* 79:085119.

35. Kitaev AY (2003) Fault-tolerant quantum computation by anyons. *Ann Phys* 303: 2–30.
36. Barrett S, Hammerer K, Harrison S, Northup TE, Osborne TJ (2013) Simulating quantum fields with cavity QED. *Phys Rev Lett* 110:090501.
37. Varnava M, Browne DE, Rudolph T (2006) Loss tolerance in one-way quantum computation via counterfactual error correction. *Phys Rev Lett* 97:120501.
38. Chu Y, et al. (2017) Quantum acoustics with superconducting qubits. *arXivorg p.* 1703.00342.